

FOUR-DIMENSIONAL Q²PSK
MODULATION AND CODING FOR
MOBILE DIGITAL COMMUNICATION

VAN WYK, DANIEL JACOBUS

DANIEL JACOBUS VAN WYK

FOUR-DIMENSIONAL Q²PSK MODULATION AND CODING
FOR MOBILE DIGITAL COMMUNICATION

Master of Engineering (Electronics)

MEng

UP

1996

ELECTRICAL AND ELECTRONIC ENGINEERING

FACULTY OF ENGINEERING

UNIVERSITY OF PRETORIA

SUPERVISOR: J. J. F. Van der Merwe

1996

FOUR-DIMENSIONAL Q²PSK MODULATION AND CODING FOR MOBILE DIGITAL COMMUNICATION

by

DANIËL JACOBUS VAN WYK

A dissertation submitted as partial fulfilment
of the requirements for the degree

Master of Engineering (Electronic)

in

ELECTRICAL AND ELECTRONIC ENGINEERING

in the

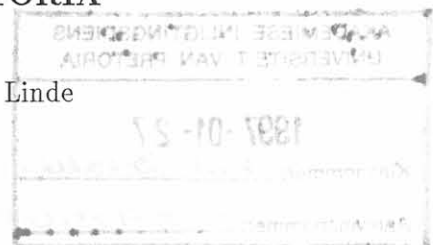
FACULTY OF ENGINEERING

at the

UNIVERSITY OF PRETORIA

SUPERVISOR: Prof. L.P. Linde

April 1996



To my wife, Daleen

For all her support and love.
Without her, this study would
not have been possible.

Key Words:

Phase-Shift Keying, Mobile Digital Communication, Multidimensional Signalling, Synchronisation and Forward Error Correction.

SUMMARY

In this dissertation an indepth research into the design, implementation and evaluation of a digital four-dimensional modem for application to high speed mobile communication on the V/UHF channel has been carried out. The four-dimensional digital signalling employs Quadrature-Quadrature Phase-Shift Keying (Q^2 PSK) as modulation scheme, which was claimed to outperform two-dimensional modulation schemes in terms of spectral efficiency. Q^2 PSK constitutes a relatively new modulation technique, and for this reason considerations of digital modulation and demodulation, synchronisation and error correction coding for this signalling scheme, are of utmost importance.

A conventional DSP based implementation of a Q^2 PSK modulator/demodulator is considered in this thesis. Furthermore, key synchronisation strategies are considered, including new carrier phase and frequency tracking loops. A novel frame synchronisation strategy for Q^2 PSK, employing complex correlation sequences, is presented. The excellent bandwidth efficiency of the Q^2 PSK signalling strategy and elegant signal structure, facilitates the incorporation of sophisticated forward error correction strategies. For this reason the dissertation introduces new trellis codes for Q^2 PSK, including classical, TCM and MTCM, for transmission over both the AWGN and mobile fading channels. Performance evaluations of the developed Q^2 PSK digital modem are given from results obtained from computer simulations when operating on the static AWGN channel and mobile Rician or Rayleigh fading channels.

The research work can be summarised as follows:

- Realisation of a digital Q^2 PSK mobile communication system simulation test facility, facilitating burst mode communication scenarios;
- Design and implementation of a novel frame synchronisation strategy employing complex correlation sequences, for the Q^2 PSK system;
- Design and implementation of a Q^2 PSK dual carrier phase and frequency Kalman estimator for carrier phase and frequency tracking;
- Novel application of classical convolutional error correction codes to Q^2 PSK. In addition, the derivation of theoretical upper bounds to bit error probability are presented;
- Design and application of trellis codes for transmission over the AWGN channel are presented;
- Design and application of multiple trellis codes for transmission over the Rician fading channel are presented with some new results;
- Not only are the extensive evaluations presented, but the performance bounds derived, are benchmarked against actual simulation curves.

ACKNOWLEDGEMENTS

I would like to thank my Creator, to Him all the praise !

I am indebted to many people for their advice and assistance towards the successful completion of this dissertation.

In particular to my supervisor, Professor Louis Linde for directing this research and his constant and enthusiastic encouragement. His superb supervision and most professional approach, in every way, has benefited me tremendously.

For financial assistance and unique opportunities I thank Armscor, the Foundation for Research Development (FRD) and the Laboratory for Advanced Engineering (LGI).

I would like to thank Professor Ezio Biglieri and Dr. Giorgio Taricco from the Politecnico Di Torino (Italy) for answering my questions and for the invaluable discussions and suggestions on TCM and MTCM.

To my research colleagues and friends Jacques Cilliers, Frans Marx, Emlyn Davies, Gert Veale, Roelf du Toit and Etiënne Pretorius my sincere thanks for being at my disposal at all times to help me with many computing and other technical problems and solutions. I would also like to thank David Joubert, previously of LGI, for his assistance and many discussions during the development of the Q²PSK modem platform. A special word of gratitude is expressed to Jacques Cilliers for the many hours of discussions on Trellis Coded Modulation and also his patience in teaching me the finer details concerning Object Oriented Programming.

To my parents, parents in-law and sisters for their unselfish support. Finally, I would also express my deepest gratitude to my wife, Daleen for her continuous support and love.

CONTENTS

GLOSSARY OF ABBREVIATIONS	v
LIST OF SYMBOLS	vii
1 INTRODUCTION	1
1.1 INTRODUCTION AND OVERVIEW	1
1.2 LITERATURE SURVEY	3
1.2.1 Multidimensional modulation	3
1.2.2 Error correction techniques	5
1.2.3 Trellis codes for Q ² PSK	7
1.3 DISSERTATION ORGANISATION	8
I FOUR-DIMENSIONAL Q ² PSK: Theory and Application to mobile communication	11
2 FOUR-DIMENSIONAL Q ² PSK SIGNALLING: THEORETICAL FOUNDATION	12
2.1 FOUR-DIMENSIONAL SIGNALLING	12
2.2 Q ² PSK SIGNALLING	14
2.2.1 Q ² PSK Modulation	15
2.2.2 Q ² PSK Demodulation	17
2.2.3 Spectral efficiency analysis of Q ² PSK	18
2.2.4 BER performance	21
2.3 ON THE CAPACITY OF Q ² PSK FOR BANDLIMITED AWGN CHANNELS	25
2.4 CONCLUDING REMARKS: CHAPTER 2	27

3	Q²PSK — MOBILE COMMUNICATION SYSTEM	29
3.1	GENERAL SYSTEM ARCHITECTURE	30
3.1.1	Transmitter	30
3.1.2	Receiver	33
3.2	FADING CHANNEL	34
3.2.1	Fading channel model	35
3.2.2	Noise in the Mobile Channel	36
3.2.3	Mobile Channel Simulator	37
3.3	SYSTEM SPECIFICATION	38
3.4	CONCLUDING REMARKS: CHAPTER 3	41
4	DIGITAL Q²PSK — Modulation, Demodulation and Synchronisation	42
4.1	MODEM REALISATION	42
4.1.1	Digital Q ² PSK Modulator	42
4.1.2	Digital Q ² PSK Demodulator	45
4.1.3	Modem waveforms and spectra	48
4.2	BLOCK TRANSMISSION STRATEGY	49
4.3	Q ² PSK SYNCHRONISATION	54
4.3.1	Frame Synchronisation	54
4.3.2	Carrier and Symbol Synchronisation	56
4.3.3	Effect of Carrier Phase and Frequency Errors on BER	58
4.3.4	Kalman Phase and Frequency Estimation	59
4.4	CONCLUDING REMARKS: CHAPTER 4	66
II	TRELLIS CODING WITH APPLICATION TO Q²PSK	67
5	DESIGN FOR AWGN CHANNELS	68
5.1	INTRODUCTION TO ERROR CORRECTION	68
5.2	CLASSICAL ERROR CORRECTION	69
5.2.1	Convolutional Channel Coding	69
5.2.2	Maximum Likelihood Decoding	71

5.2.3	Performance Estimates	73
5.3	TRELLIS CODED MODULATION	76
5.3.1	Rate 3/4 Q ² PSK/TCM	80
5.3.2	Rate 2/4 Q ² PSK/TCM	82
5.3.3	Q ² PSK/TCM code performance	84
5.3.4	Analytical upper performance bounds for Q ² PSK/TCM	85
5.4	CONCLUDING REMARKS: CHAPTER 5	86
6 DESIGN OF TCM AND MTCM FOR FADING CHANNELS 88		
6.1	MULTIPLE TRELLIS CODED MODULATION	89
6.1.1	Ungerboeck Set Partitioning: From <i>Root-to-Leaf</i>	90
6.2	Q ² PSK/MTCM CODE DESIGN	94
6.2.1	Design of 4-State Rate 6/8 codes	94
6.3	PERFORMANCE ANALYSIS	95
6.3.1	TCM for fading channels	95
6.3.2	MTCM for fading channels	96
6.4	CONCLUDING REMARKS: CHAPTER 6	96
III Q²PSK Modulation and Coding: PERFORMANCE EVALUATION 98		
7 PERFORMANCE EVALUATION 99		
7.1	INTRODUCTION	99
7.1.1	SNR versus E_b/N_o	99
7.1.2	Simulation software	101
7.2	EVALUATION ON AWGN CHANNELS	101
7.2.1	Mobile Channel effects in AWGN	105
7.2.2	Phase/Frequency Tracking and Correction	111
7.2.3	DSP implementation	113
7.2.4	Classical and TCM error correction in AWGN	115
7.3	EVALUATION ON FADING CHANNELS	118
7.3.1	Trellis Coded Q ² PSK	124
7.4	CONCLUDING REMARKS: CHAPTER 7	127

8	CONCLUSIONS AND FUTURE RESEARCH	129
8.1	FUTURE RESEARCH	130
8.1.1	Design and implementation of a multidimensional equaliser	130
8.1.2	Application of a burst-error correcting Viterbi decoder	131
8.2	Design of Ungerboeck-type codes for fading channels	131
8.3	CONCLUDING REMARKS: CHAPTER 8	132
A	A TUTORIAL ON TCM	135
A.1	INTRODUCTION	135
A.1.1	Fundamentals of TCM	136
A.2	HEURISTIC AND ANALYTIC REPRESENTATION OF TCM	138
A.2.1	Ungerboeck Codes	138
A.2.2	Calderbank—Mazo Codes	139
A.3	PERFORMANCE EVALUATION	140
A.3.1	Analytical Upper Bound to the Error Probability of Q ² PSK	140
A.3.2	Lower Bound to Error Probability	142
A.3.3	Union Bound techniques	142
A.4	DECODING TCM	143
A.5	CONCLUDING REMARKS: APPENDIX A	145
B	TCM CODE DESIGN — Utility Software	146
B.1	Calderbank—Mazo Description of trellis codes	146
B.2	Mulligan—Wilson Algorithm for computation of d_{free}	150
C	TRANSFER FUNCTION DERIVATION	156
D	SET PARTITIONING FOR Q²PSK/MTCM CODE DESIGN	159
D.1	CODE CARDINALITY OF 16	159
D.2	CODE CARDINALITY OF 8	161

GLOSSARY OF ABBREVIATIONS

1D	— One-Dimensional
2D	— Two-Dimensional
4D	— Four-Dimensional
ACI	— Adjacent Channel Interference
AFC	— Automatic Frequency Control
ASK	— Amplitude-Shift Keying
AWGN	— Additive White Gaussian Noise
B-E	— Bandwidth-Efficiency
BEP	— Bit Error Probability
BER	— Bit Error Rate
BPF	— Bandpass Filter
BSC	— Binary Symmetric Channel
CC	— Cross-Correlation
CCI	— Co-Channel Interference
CCRM8	— Convolutional Codes over Ring Modulo-8
CDMA	— Code-Division Multiple-Access
CE-Q ² PSK	— Constant Envelope Q ² PSK
C/N	— Carrier-to-Noise Ratio
CSI	— Channel State Information
DPFKE	— Dual Phase-Frequency Kalman Estimator
DMC	— Discrete Memoryless Channel
DS	— Distance Spectrum
DSP	— Digital Signal Processing
EEP	— Error Event Path
ED	— Euclidean Distance
EKF	— Extended Kalman Filter
EM	— Electromagnetic
E-E	— Energy-Efficiency
FDMA	— Frequency-Division Multiple-Access
FEC	— Forward Error Correction
FH	— Frequency Hopped
FPM	— Frequency Phase Modulation
FIR	— Finite Impulse Response
FSK	— Frequency-Shift Keying
GMSK	— Gauss Minimum-Shift Keying
HT	— Hilbert Transform(er)
IF	— Intermediate Frequency
ISI	— Intersymbol Interference

LCR	— Level Crossing Rate
LMC	— Land Mobile Channel
LMSC	— Land Mobile Satellite Channel
LO	— Local Oscillator
LOS	— Line-of-Sight
LPF	— Lowpass Filter
M-PSK	— M-ary Phase-Shift Keying
MED	— Minimum Euclidean Distance
MFD	— Mean Fade Duration
ML	— Maximum Likelihood
MSE	— Minimum Square Error
MSED	— Minimum Squared Euclidean Distance
MSK	— Minimum Shift-Keying
MTCM	— Multiple Trellis-Coded Modulation
NEP	— Negative Equally Probable
PCS	— Personal Communication Services
PDF	— Probability Density Function
PLL	— Phase-Locked Loop
PSK	— Phase-Shift Keying
PSD	— Power Spectral Density
QASK	— Quadrature Amplitude-Shift Keying
QPSK	— Quadrature Phase-Shift Keying
$\pi/4$ -QPSK	— $\pi/4$ Quadrature Phase-Shift Keying
Q ² PSK	— Quadrature-Quadrature Phase-Shift Keying
Q ² PSK/TCM	— Trellis Coded Q ² PSK
Q ² PSK/MTCM	— Multiple-Trellis Coded Q ² PSK
RHS	— Right Hand Side
RI	— Rotational Invariant
RF	— Radio Frequency
SEP	— Symbol Error Probability
SFH	— Slow Frequency Hopping
SKF	— Scalar Kalman Filter
SNR	— Signal-to-Noise Ratio
S/P	— Serial-to-Parallel
TCM	— Trellis-Coded Modulation
TDMA	— Time-Division Multiple-Access
VA	— Viterbi Algorithm
V/UHF	— Very- and Ultra-High Frequency

LIST OF SYMBOLS

C	— Channel capacity
D	— Dimensions per second
d_{free}	— Minimum Euclidean Distance
d_{free}^2	— Minimum Squared Euclidean Distance
η_f	— Bandwidth Efficiency (<i>bits/s/Hz</i>)
E_b/N_o	— Ratio of Energy per bit to Noise spectral density
f	— Frequency
f_c	— Carrier frequency (<i>Hz</i>)
f_d	— Deviation frequency (<i>Hz</i>)
f_D	— Doppler frequency (<i>Hz</i>)
f_e	— Frequency error
G_c	— Coding gain
γ_c	— Asymptotic coding gain
h	— Deviation ratio
k	— MTCM multiplicity
K	— Rician factor
L_c	— Constraint length
M	— Number of symbols per signal set
N	— Dimensionality
N_s	— Number of trellis coder states
P_b	— Bit Error Probability
P_s	— Symbol Error Probability
ψ_i	— i -th Orthonormal basis
Q	— Number of quantisation bits
R_b	— Bit Rate (<i>bits/s</i>)
R_c	— Code rate (k/n)
R_s	— Symbol Rate (<i>Symbols/s</i>)
$s(t)$	— Function of time
$S(f)$	— Function of frequency
t	— Time (<i>seconds</i>)
T_b	— Bit Duration (<i>seconds</i>)
T_s	— Symbol Duration (<i>seconds</i>)
$T(D)$	— Transfer function
θ_e	— Phase error (<i>radians</i>)
θ_D	— Doppler angle (<i>radians</i>)
θ_o	— Phase offset (<i>radians</i>)
W	— Bandwidth (<i>Hz</i>)

LIST OF FIGURES

1.1	Modulator with 2D/Polarisation and frequency-reuse.	4
1.2	Dissertation organisation.	8
2.1	16-ary constellations in Two-Dimensions (2D): (a) Optimal 16-ary design. (b) Standard 16-QASK design.	13
2.2	Quadrature-Quadrature Phase-Shift Keying (Q ² PSK) modulator.	15
2.3	Power spectral densities of MSK, QPSK and Q ² PSK modulated signals.	20
2.4	Power captured as function of bandwidth of MSK, QPSK and Q ² PSK signals.	20
2.5	Power spectral densities of Q ² PSK, CP-Q ² PSK and 4-CPFSK modulated signals.	22
2.6	Power captured as function of bandwidth for Q ² PSK and CP-Q ² PSK signals.	22
2.7	Signals on vertices of $N = 3$ dimensional hypercube.	24
2.8	Channel capacity C^* of 2D M-PSK ($M = 4, 8$ and 16 , denoted by dashed lines) and 4D Q ² PSK modulation for bandlimited AWGN channels.	26
3.1	Basic communication system model.	30
3.2	Detailed transmitter block diagram.	31
3.3	Detailed receiver block diagram.	33
3.4	Non-frequency selective Rician fading channel model.	35
3.5	V/UHF mobile channel simulator block diagram.	37
3.6	Power spectral density of fading process when an omnidirectional antenna is employed.	38
3.7	Overall radio channel response.	39
4.1	Q ² PSK Transmitter block diagram.	43
4.2	Fourier Transform of basic data pulse, $a(t)$; with amplitude ± 1 , width T_s , and centered on the origin.	44
4.3	Visualisation of first quadrature modulation in the frequency domain, producing in-phase digital signal, $I(nT_{smp})$	44
4.4	Visualisation of final modulation process in the frequency domain, producing Q ² PSK transmitter output, $s(nT_{smp})$	45

4.5	Q ² PSK DSP based receiver block diagram	46
4.6	Non-optimum demodulator decision devices for (a) Q ² PSK, and (b) CE-Q ² PSK.	48
4.7	Decoupled Q ² PSK signal space.	49
4.8	An illustrative timing diagram showing the waveforms involved in generating the Q ² PSK signal.	50
4.9	An illustrative timing diagram showing the waveforms involved in generating the CE-Q ² PSK signal.	50
4.10	Power spectral densities of Q ² PSK, CE-Q ² PSK and CP-Q ² PSK.	51
4.11	Basic frame structure.	52
4.12	Block signalling format for symbol rate of $R_s = 5.0 \text{ ksymbols/s}$ for the different hopping rates, (a) 25 (b) 50 (c) 100 <i>hops/s</i> , utilising an 8 symbol header.	53
4.13	Proposed Q ² PSK frame synchronisation procedure.	55
4.14	Complex correlator block diagram.	56
4.15	Saha synchronisation circuit for Q ² PSK.	57
4.16	Saha synchronisation circuit for CE-Q ² PSK.	57
4.17	BEP sensitivity of Q ² PSK to a Tikhonov-distributed phase error.	60
4.18	Optimum recursive scalar Kalman estimator.	62
4.19	Dual Frequency and Phase Kalman Estimator (DPFKE).	64
5.1	Rate-3/4 encoding scheme for Q ² PSK.	70
5.2	Half rate encoding scheme for Q ² PSK.	70
5.3	Half rate encoding scheme for CE-Q ² PSK.	71
5.4	Decoding scheme for rate-3/4 Q ² PSK.	72
5.5	Decoding scheme for rate-1/2 Q ² PSK.	72
5.6	Decoding scheme for rate-1/2 CE-Q ² PSK.	73
5.7	Bit error probability, P_b for Rate-1/2 codes with Viterbi decoding (Hard quantisation) and Q ² PSK modulation.	74
5.8	Bit error probability for Rate-2/3 codes with Viterbi decoding (Hard quantisation) and Q ² PSK modulation.	75
5.9	Bit error probability for Rate-3/4 codes with Viterbi decoding (Hard quantisation) and Q ² PSK modulation.	75
5.10	Group $B_0 = \{C_0, C_1, C_2, C_3\}$: Even Parity	78
5.11	Group $B_1 = \{C_4, C_5, C_6, C_7\}$: Odd Parity	79
5.12	Q ² PSK signal space partition tree.	80

5.13	Inputs and state variables for the half-connected 8-state code.	81
5.14	Half-connected $R = 3/4$ 8-state trellis code.	81
5.15	Inputs and state variables for fully-connected 8-state code.	82
5.16	Fully-connected $R = 3/4$ 8-state trellis code.	82
5.17	Code structures for half-rate trellis coders.	83
5.18	Half-connected $R = 2/4$ 8-state trellis code.	83
5.19	Quarter-connected $R = 2/4$ 16-state trellis code.	84
5.20	Half-connected $R = 2/4$ 8-state trellis code for Constant Envelope (CE) Q ² PSK. . .	85
5.21	Upper bounds to bit error probabilities for 8-state rate-3/4 Q ² PSK/TCM.	86
6.1	Generalised MTCM transmitter.	89
6.2	Set partitioning method for multiple ($k = 2$) trellis codes on the fading channel. . . .	93
6.3	Set partitioning method for multiple ($k = 4$) trellis codes on the fading channel. . . .	93
6.4	Rate-6/8 4-state Q ² PSK/MTCM	94
7.1	Power spectral densities of unfiltered and filtered Q ² PSK (CE-Q ² PSK).	101
7.2	Q ² PSK operating at 2.0 <i>bits/s/Hz</i> in AWGN with $E_b/N_o = 25.0$ dB.	102
7.3	Q ² PSK operating at 2.0 <i>bits/s/Hz</i> in AWGN with $E_b/N_o = 5.0$ dB.	102
7.4	Q ² PSK signal under static channel conditions (X-axis: samples, Y-axis: volt).	103
7.5	CE-Q ² PSK signal under static channel conditions.	103
7.6	BEP curves for MSK, QPSK, Q ² PSK, and CE-Q ² PSK.	104
7.7	BEP curves for Q ² PSK and CE-Q ² PSK, operating at 2.0 and 2.4 <i>bits/s/Hz</i> , respectively.	105
7.8	Q ² PSK signal constellations for phase offset, $\theta_o = 0.05$ rad.	106
7.9	Q ² PSK signal constellations for phase offset, $\theta_o = 0.1$ rad.	106
7.10	Q ² PSK signal constellations for phase offset, $\theta_o = 0.2$ rad.	106
7.11	Q ² PSK signal constellations for Doppler frequency of 25 <i>Hz</i> at RF frequency of 900 <i>MHz</i>	107
7.12	Q ² PSK signal constellations for Doppler frequency of 50 <i>Hz</i>	107
7.13	Q ² PSK signal constellations for Doppler frequency of 100 <i>Hz</i>	107
7.14	CE-Q ² PSK signal constellations for phase offset, $\theta_o = 0.01$ rad.	108
7.15	CE-Q ² PSK signal constellations for phase offset, $\theta_o = 0.1$ rad.	108
7.16	CE-Q ² PSK signal constellations for phase offset, $\theta_o = 0.2$ rad.	108

7.17	CE-Q ² PSK signal constellations for Doppler frequency of 25 Hz at RF frequency of 900 MHz.	109
7.18	CE-Q ² PSK signal constellations for Doppler frequency of 50 Hz.	109
7.19	CE-Q ² PSK signal constellations for Doppler frequency of 100 Hz.	109
7.20	BEP curves for Q ² PSK for $\theta_o = 0.1$ rad and Doppler frequencies of 25, 50 and 100 Hz, compared to the ideal Q ² PSK modem transmission in AWGN.	110
7.21	BEP curves for CE-Q ² PSK for $\theta_o = 0.1$ rad and Doppler frequencies of 25, 50 and 100 Hz, compared to the ideal CE-Q ² PSK modem transmission in AWGN.	110
7.22	Minimum Squared Errors for DPFKE estimator tracking carrier phase and frequency uncertainties over the header period (a) Frequency MSE, ρ_k (b) Phase MSE, ρ_l	112
7.23	Frequency MSE for DPFKE estimator tracking carrier frequency uncertainties over the data period.	112
7.24	BEP curves for Q ² PSK and CE-Q ² PSK with DPFKE activated.	113
7.25	Q ² PSK constellations (cosine-carrier information) under static AWGN channel conditions (a) $E_b/N_o = 20.0$ dB (b) $E_b/N_o = 15.0$ dB.	114
7.26	Q ² PSK constellations (cosine-carrier information) under mobile channel impairments for $E_b/N_o = 25$ dB (a) carrier phase offset $\theta_o = 0.1$ rad (b) Doppler frequency $f_D = 100.0$ Hz.	114
7.27	Q ² PSK constellations for a constant phase offset $\theta_o = 0.1$ rad, a Doppler frequency $f_D = 50.0$ Hz and $E_b/N_o = 15.0$ dB (a) cosine-carrier information (b) cosine-sine-carrier information.	115
7.28	BEP graphs 8- and 16-state rate-2/4 Q ² PSK, compared to uncoded Q ² PSK and the upper bounds to BEP.	116
7.29	BEP graphs 8- and 16-state hybrid rate-2/4 Q ² PSK employing a single rate-2/3 convolutional coder, compared to uncoded CE-Q ² PSK and the upper bounds to BEP.	116
7.30	BEP graphs 8- and 16-state rate-3/4 Q ² PSK employing a single rate-3/4 convolutional coder, compared to uncoded Q ² PSK and the upper bounds to BEP.	117
7.31	BEP graphs 8- and 16-state rate-2/4 Q ² PSK/TCM and CE-Q ² PSK/TCM compared to uncoded Q ² PSK.	119
7.32	BEP graphs 8- and 16-state rate-3/4 Q ² PSK/TCM, compared to uncoded Q ² PSK.	119
7.33	Q ² PSK under Rician fading channel conditions, $K = 10$ dB.	120
7.34	CE-Q ² PSK under Rician fading channel conditions, $K = 10$ dB.	120
7.35	Q ² PSK under Rayleigh fading channel conditions, $K = 0$ dB.	121
7.36	CE-Q ² PSK under Rayleigh fading channel conditions, $K = 0$ dB.	121
7.37	Q ² PSK operating at 2.0 bits/s/Hz under Rician fading channel conditions with $K = 5$ dB and $E_b/N_o = 25$ dB.	122
7.38	Q ² PSK operating at 2.0 bits/s/Hz under Rayleigh fading channel conditions with $K = 0$ dB and $E_b/N_o = 25$ dB.	122

7.39	BER results for Q ² PSK modem operating on AWGN, Rician and Rayleigh fading channel.	123
7.40	BER results for CE-Q ² PSK modem operating on AWGN, Rician and Rayleigh fading channel.	123
7.41	BER results for 4-state rate-6/8 and rate-5/8 Q ² PSK/MTCM operating on Rician ($K = 10$ dB) fading channel.	125
7.42	BER results for 4-state rate-6/8 and rate-5/8 Q ² PSK/MTCM modem operating on Rician ($K = 5$ dB) fading channel.	125
7.43	BER results for 4-state rate-5/8 Q ² PSK/MTCM modem operating on Rician ($K = 5$ dB) fading channel without and with CSI based on the correlation-magnitude of the frame and symbol synchronisation process.	126
A.1	General model for TCM.	137
A.2	Block diagram of an Ungerboeck code ($m = \log_2 M$).	138
A.3	General structure of the Calderbank—Mazo analytical description	139
C.1	Fully-connected $R = 3/4$ 8-state trellis code.	157

LIST OF TABLES

2.1	Comparison of required SNR to achieve a symbol-error probability, $P_s = 10^{-5}$	26
2.2	Bandwidth comparison of MSK, QPSK, 4-CPFSK, Q ² PSK and CP-Q ² PSK signalling as a function of power containment.	27
3.1	Channel specifications	39
3.2	Modem specifications	40
4.1	Block transmission format for hopping rates of $R_{HOP} = 25, 50$, and 100 hops/s	52
4.2	SFH design summary for hopping rates of $R_{HOP} = 25, 50$, and 100 hops/s	53
5.1	Minimum squared Euclidean distances between all pairs of Q ² PSK code words. . . .	77
6.1	Interdistances between partitioned subsets, with $A_0 \otimes B_0$ used as reference.	91
6.2	Interdistances between partitioned subsets, with $C_0 \otimes D_{0a}$ used as reference.	92
6.3	Design summary for Q ² PSK/MTCM.	95
7.1	Comparison of trellis codes for Q ² PSK at a BEP of $P_e = 10^{-5} \text{ dB}$	127